JOURNAL OF MATERIALS SCIENCE **39** (2004) 6257–6262

Optical properties of SPS-ed Y- and (Dy,Y)-α-sialon ceramics

XINLU SU, PEILING WANG*, WEIWU CHEN
The State Key Lab of High Performance Ceramics and Superfine Microstructure, Shanghai Institute of Ceramics, Chinese Academy of Sciences, Shanghai 200050, People's Republic of China
E-mail: plwang@sunm.shcnc.ac.cn

ZHIJIAN SHEN, M. NYGREN
Department of Inorganic Chemistry, University of Stockholm, S-106 91 Stockholm, Sweden

YIBING CHENG
School of Physics and Materials Engineering, Monash University, Clayton, Victoria 3800, Australia

DONGSHENG YAN
The State Key Lab of High Performance Ceramics and Superfine Microstructure, Shanghai Institute of Ceramics, Chinese Academy of Sciences, Shanghai 200050, People's Republic of China

$Y_{0.67}Si_9Al_3ON_{15}$ and $Dy_{0.4}Y_{0.3}Si_{8.85}Al_{3.15}O_{1.05}N_{14.95}$ ceramics were prepared by Spark Plasma Sintering (SPS) with and without heat treatment at 1700°C for 7 h or 17 h, and their optical transmittance were investigated over the wavenumber range 4000–1500 cm^{-1}. The results showed that the assemblages of the SPS-ed samples consisted of single crystallized α-sialon phase in both compositions. EDS analysis indicated that α-sialon was mainly stabilized by Dy^{3+} in the multi-cation (Dy,Y)-α-sialon composition. The SPS-ed specimens showed relatively high optical transmission properties, and the maximum transmittance reached around 65% at 2800 cm^{-1} for 0.5 mm thick specimens of both compositions. The 7 h heat treatment caused the formation of small amount of melilite phase, resulting in non-uniform microstructure and decrease in optical transmittance. Extended heat treatment for 17 h led to more homogenous microstructure and increased the transmittance to some extent. Less melilite was formed in the multi-cation (Dy,Y)-α-sialon composition than in the single cation Y-α-sialon after heat treatment, and the transmittance of (Dy,Y)-α-sialon was also higher than that of Y-α-sialon.

1. Introduction

α-sialon (abbreviated as α'), a solid solution of α-Si_3N_4, has a general composition expressed as $M_xSi_{12-(m+n)}Al_{(m+n)}O_nN_{16-n}$ [1], where M represents Li, Ca, Mg, Y and some lanthanide elements [2–4]. In comparison to Si_3N_4, α' material offers advantage of easier fabrication because of the lower viscosity of the M-Si-Al-O-N liquid phase formed during sintering. Another advantage of α' is the ability to reduce the amount of residual glassy phase as the α' phase can incorporate the stabilizing element into its structure together with the substitution of Al and O for part of Si and N. Furthermore, α' exhibits higher hardness and better thermal shock resistance than β-sialon.

Although there are only a limited number of studies on the optical properties of sialon ceramics [5–7], α' with high optical transparency attracts our attention. It is considered that the application field of sialon ceramics would be broadened, for example used in optical window and missile dome at high temperature or under severe conditions, if they can be prepared with high optical transparency. The present work focused on Y-α' and multi-cation (Dy,Y)-α' systems and studied the effects of stabilizer in the compositions and different thermal treatment time with fixed temperature on the optical transmission of α' ceramics at wavenumbers 4000–1500 cm^{-1}. All samples were prepared by spark plasma sintering (SPS), a rapid consolidation technique, to ensure high density. Subsequent heat treatment was performed on these samples and its influence on the optical properties of α' ceramics was studied.

*Author to whom all correspondence should be addressed.

2. Experimental

Two compositions, $Y_{0.67}Si_9Al_3ON_{15}$ and $Dy_{0.4}Y_{0.3}Si_{8.85}Al_{3.15}O_{1.05}N_{14.95}$, (named as Y67 and Dy4Y3 respectively) used in this study lie on the Si_3N_4-9AlN:Y_2O_3 ($m = 2n$) tie line of the α' plane in the system of M-Si-Al-O-N (M = Y or Dy/Y) according to the formula of $R_{m/3}Si_{12-(m+n)}Al_{m+n}O_nN_{16-n}$.

Starting powders of α-Si_3N_4 (SN-10, UBE Industries, Japan, 1.3 wt%O), AlN (Wuxi Chemical Plant, China, 1.3 wt%O), Dy_2O_3 (99.9%, Yaolong Chemical Plant, China) and Y_2O_3 (99.99%, Yaolong Chemical Plant, China) were milled in absolute alcohol for 24 h in a plastic jar, using sialon milling media, and then dried under an infrared lamp. The oxygen content on the surface of Si_3N_4 and AlN was not taken into account when calculating the starting compositions. This is because the compositions consisted of α-Si_3N_4, AlN and Dy_2O_3/Y_2O_3 with the different molecular ratios, and the compensation of oxygen content is difficult to be made without Al_2O_3 as the starting material, implying that these two compositions would be shifted towards the side of oxygen rich. Pellets of dried powders were sintered under nitrogen atmosphere in a Dr. Sinter 1050 Spark Plasma Sintering (SPS) apparatus (Sumitomo Coal Co. Ltd., Japan). Compacts were placed between two carbon rams in a cylindrical carbon die with an inner diameter of 20 mm. The pellets were heated at a rate of 100°C/min under 50 MPa between the rams. The temperature during SPS was measured by infrared thermometer, which is similar to the method of temperature measurement used in hot pressing. The shrinkage and shrinkage rate of specimen were recorded by monitoring the displacement of the rams. When no sample shrinkage was detected, the temperature was held constant for 75 s before the power was shut off. Heat treatment was carried out at 1700°C for 7 and 17 h respectively in a graphite resistance furnace under protective nitrogen atmosphere.

Bulk densities of specimens were measured by the Archimedes principle. Phase assemblages were determined by XRD using a Guinier-Hägg camera with Cu $K_{\alpha 1}$ radiation and Si as an internal standard. The measurement of X-ray film and refinement of lattice parameters were completed by a computer-linked line scanner (LS-18) [8] system and the program PIRUM [9]. Microstructure observation of the specimens was performed under a field emission Scanning Electronic Microscope (Jeol JSE-6700F) equipped with an energy dispersive X-ray spectrometer (EDS) (Oxford/LINK ISIS 3.00). Optical transmissions at wavenumbers 4000–1500 cm^{-1} (2.5–6.6 μm) were measured by FT-IR (NICOLET NEXUS).

3. Results and discussion

The sintering temperatures for obtaining densified Y67 and Dy4Y3 were 1600°C. The direct experiment and numerical simulation have shown that in the condition applied in SPS experiment the temperature inside the die is higher than what measured by the pyrometer, such a difference is about 100°C [10, 11]. By counting in this difference the temperature required for SPS appears lower than what required by, for instance, conventional hot pressing. The enhanced densification in SPS has been ascribed to the non-equilibrium nature of the process [12]. Bulk densities of SPS-ed Y67 and Dy4Y3 are 3.37 and 3.55 g/cm^3 respectively. The 7 and 17 h heat treatment did not induce a significant change in the bulk densities of the specimens, as listed in Table I. Single α' phase was obtained for both compositions by SPS with a holding time of only 75 s, as confirmed by the XRD analysis. Heat treatment at 1700°C for 7 h led to the formation of a small amount of a second crystalline melilite phase in both compositions, although the melilite content was higher in Y67 than in Dy4Y3. Extending the heat treatment time to 17 h did not increase the amount of melilite phase in Y67, and decreased the melilite content in Dy4Y3. Table I also lists the cell dimensions of α' phase for both SPS-ed and heat treated samples. The lattice parameters of α' phase in SPS-ed Dy4Y3 is larger than that in SPS-ed Y67, which is attributed to the slightly higher x value in the composition of Dy4Y3 than that in Y67, and the larger ionic radius of Dy^{3+} than Y^{3+}. According to the empirical equations for the unit cell dimension of α' in the Y-containing α' [13], the lattice parameters a and c corresponding to $m = 2.0$ ($n = 1.0$) would be about 7.851 and 5.725 Å respectively, which are just little larger than the values of a(7.840 Å) and c(5.718 Å) of Y67 measured based on XRD film data (see Table I). On the other hand, the measured lattice parameters a and c correspond to $m \sim 1.97$ and $n \sim 0.94$ respectively [13], thus implying the effect of the shift of composition from the intended one resulted from the oxygen content of the starting powders on the presence of a substantial amount of residual grain boundary phase could be

TABLE I Bulk densities, phase assemblages of specimens and cell dimensions of α' phase

Starting composition	Sintering procedure[a]	Bulk density (g/cm^3)	Phase assemblage[b]		Unit cell dimensions		
			α'	M	a (Å)	c (Å)	V (Å^3)
Y67	SPS	3.37	s		7.840(1)	5.718(1)	304.35
	SPS+HT 7 h	3.38	s	w	7.830(1)	5.711(1)	303.23
	SPS+HT 17 h	3.39	s	w	7.830(1)	5.710(1)	303.12
Dy4Y3	SPS	3.55	s		7.843(1)	5.721(1)	304.80
	SPS+HT 7 h	3.56	s	vw	7.836(1)	5.717(1)	304.04
	SPS+HT 17 h	3.57	s	tr	7.836(1)	5.716(1)	303.92

[a]SPS = Spark plasma sintering, HT = Heat treatment at 1700°C.
[b]α' = α-sialon, M = melilite, s = strong, w = weak, vw = very weak, tr = trace.

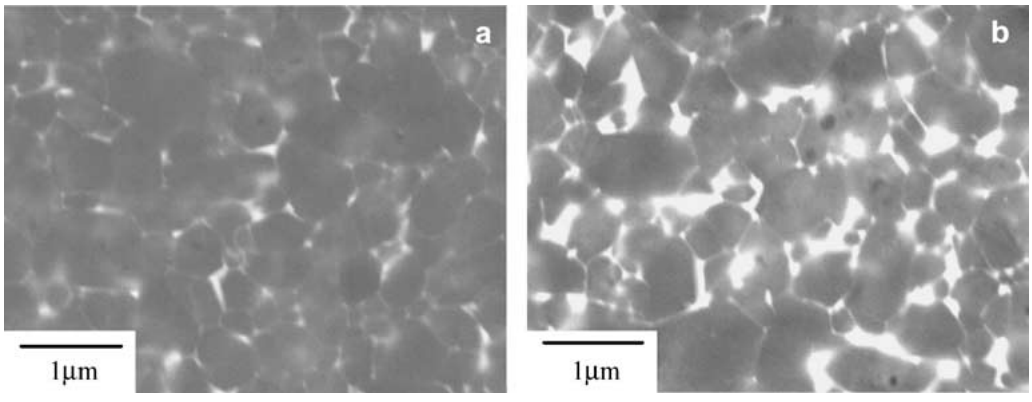

Figure 1 SEM micrographs by back-scattering mode of: (a) SPS-ed Y67 specimen and (b) SPS-ed Dy4Y3 specimen.

ignored. The cell dimensions of the α' phase decreased in both Y67 and Dy4Y3 samples after heat treatment for 7 h. However, the decrease in unit cell dimensions of the α' phase was larger in Y67 than in Dy4Y3, implying more cations entered into the grain boundary phase from the α' phase in Y67, thus crystallizing with constituents in the glass as melilite phase. When the heat treatment time was increased from 7 to 17 h, the cell dimensions of α' phase in each sample were constant within the range of deviation.

The micrographs in back-scattering mode of SPS-ed Y67 and Dy4Y3 specimens are shown in Fig. 1. It is observed that α' grains around the size of 0.4–0.8 μm are homogeneously distributed in the SPS-ed Y67 sample and a very small amount of grain boundary glassy phase can be seen by the white area in the micrograph because of enrichment of Y. In contrast, the size distribution of α' grains in Dy4Y3 sample is less uniform and a larger amount of intergranular glassy phase can be found in Dy4Y3 compared to Y67. Fig. 2a is the micrograph of Dy4Y3 after 7 h heat treatment in back scattering mode. The difference in SEM images of Dy4Y3 before and after heat treatment is obvious, as shown in Fig. 1b and Fig. 2a respectively. The gray colored phase was more uniformly distributed after heat treatment. The white colored phase could have been formed due to the intergranular accumulation of heavy atoms, such as Dy and Y, and subsequent crystallization. The XRD analysis indicated the gray regions in the figure to be mainly composed of α' and the white regions to be grain boundary melilite phase and intergranular glassy phase. Some dark regions with elongated shape were also observed in the micrograph, which may result from another crystallized phase. However, its identity could not be

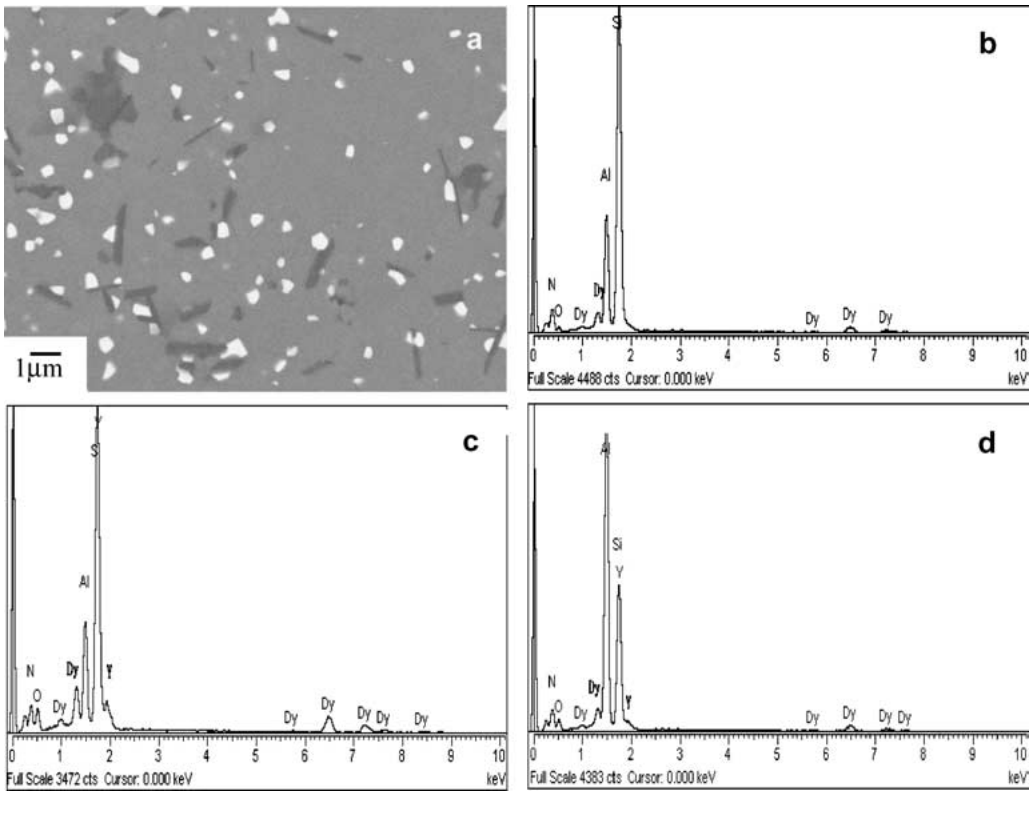

Figure 2 SEM micrographs by back-scattering mode of: (a) SPS-ed Dy4Y3 specimen after heat treatment at 1700°C for 7 h, (b) EDS pattern of α', (c) EDS pattern of melilite phase and (d) EDS pattern of AlN-polytypoids.

determined by XRD because of its low phase content. EDS was used to analyze the elemental distribution of the gray, white and dark regions in the SEM micrograph. The EDS patterns in Fig. 2b and c are consistent with the elemental distribution of α' and melilite phases respectively. The EDS spectrum obtained from one of the darker areas, is close to the AlN-polytypoids phase, if Dy^{3+} can be excluded. The solubility of Mg^{2+} and Sr^{2+}in AlN-polytypoids phase has been reported [14], but there has been no literature on Dy^{3+}incorporated AlN-polytypoids. Further work regarding the analysis of this phase is needed. It is noted that only Dy^{3+}, not Y^{3+}, was detected in the gray region of the SEM image, as shown in EDS pattern of Dy4Y3 sample in Fig. 2b. The selective solubility of cations in multi-cation α' has been reported, in which one cation, having high solubility in the α' structure, would dominant in stabilizing the α' phase and another one with low solubility mainly remained in the grain boundary [15–18]. It is not the case for the present situation, however, as Dy^{3+} has similar solubility and ionic radius to that of Y^{3+}. The reason for this result is unclear. On the other hand, both Dy^{3+} and Y^{3+} were present in the melilite phase, as confirmed by EDS on the white region of the SEM image. Fig. 3 show the SEM micrograph of Dy4Y3 after being heat treated for 17 h and the corresponding EDS patterns taken from the gray, white and dark regions of the SEM image. No significant change was observed in the SEM images by extending the heat treatment time from 7 to 17 h, except that the white area was increased, probably due to the diffusion of heavy atoms with extended holding at high temperature. On the other hand, both $Dy^{3+}$and Y^{3+} contents in melilite and Dy^{3+} content in AlN-polytypoids phase were slightly decreased according to EDS results, while the elemental analysis of α', including the result of absence of Y^{3+} in α' grains, was similar to that following the 7 h heat treatment.

TABLE II The maximum values of optical transmission of SPS-ed α-sialon specimens with and without heat treatment

	Maximum of optical transmission (%)		
Sample	SPS-ed	Heat treat-ed for 7 h	Heat treat-ed for 17 h
Y67	66	47	56
Dy4Y3	64	56	66

SEM micrographs in secondary electron mode were also taken on etched Y67 samples in order to better understand the α' grain growth during heat treatment, as shown in Fig. 4. The grain size of α' in SPSed Y67 was 0.4–0.8 μm (see Fig. 4a). Following a 7 h heat treatment, the size distribution of α' grains became inhomogeneous; equi-axed and elongated grains co-existed in the specimen, with the size of some of them being less than 0.5 μm, while some being larger than 2.0 μm (see Fig. 4b). The 17 h heat-treated specimen exhibited a more homogeneous size distribution of α' grains, with mostly equi-axed morphology and larger than 1.0 μm grain size (see Fig. 4c).

Fig. 5 show the optical transmittance curves (4000–1500 cm^{-1}) of SPS-ed Dy4Y3 and Y67 specimens with 0.50 mm thickness and heat treated for 7 and 17 h respectively. The maximum optical transmittances of SPS-ed Dy4Y3 and Y67 with and without heat treatment are listed in Table II. Before heat treatment, the

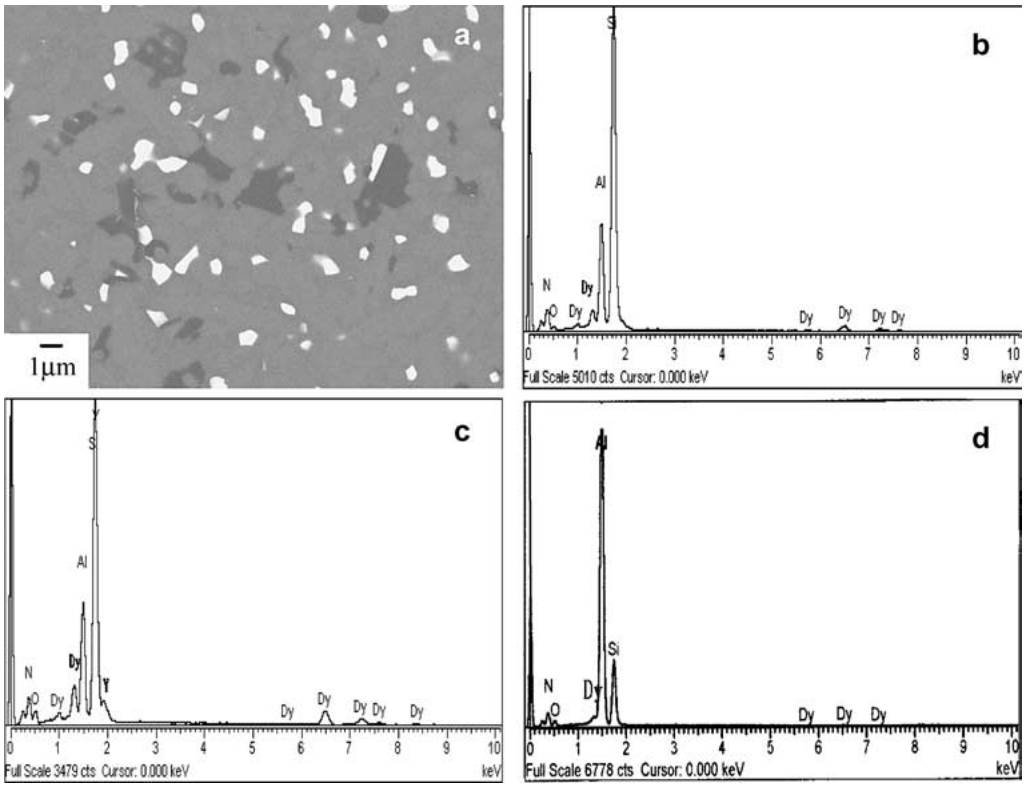

Figure 3 SEM micrographs by back-scattering mode of: (a) SPS-ed Dy4Y3 specimens after heat treatment at 1700°C for 17 h, (b) EDS pattern of α', (c) EDS pattern of melilite phase and (d) EDS pattern of AlN-polytypoids.

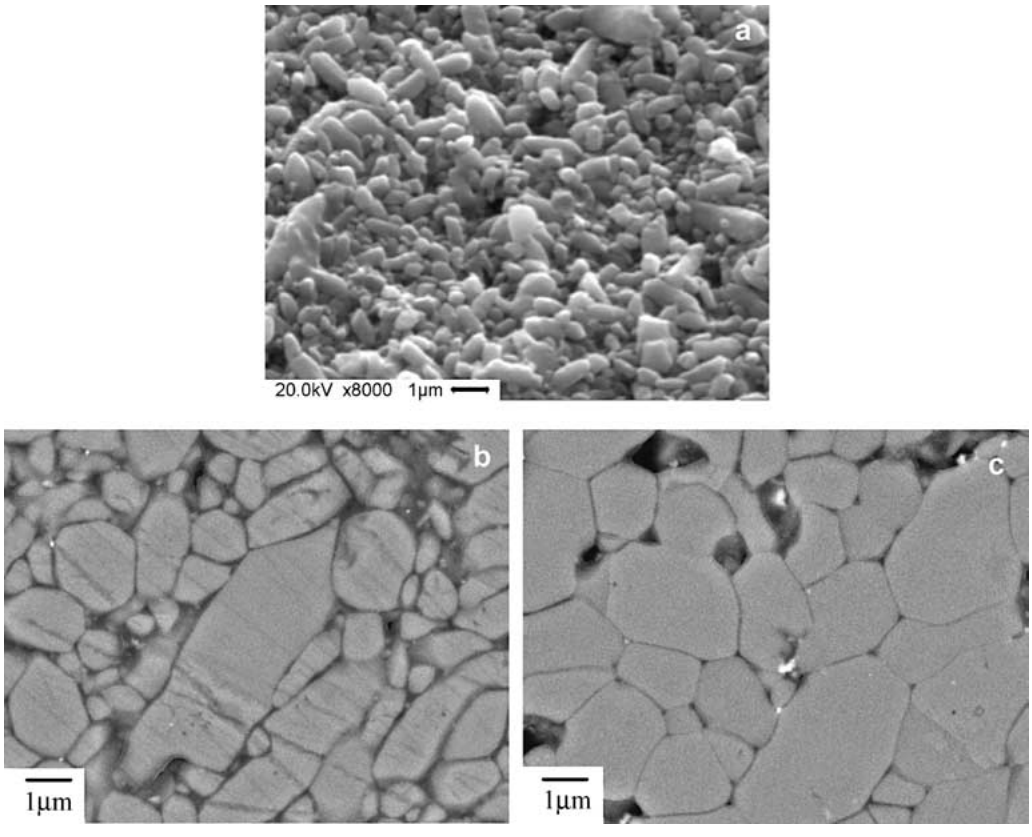

Figure 4 Micrographs of: (a) SPS-ed Y67 specimen, (b) SPS-ed Y67 + heat treatment for 7 h and (c) SPS-ed Y67 + heat treatment for 17 h.

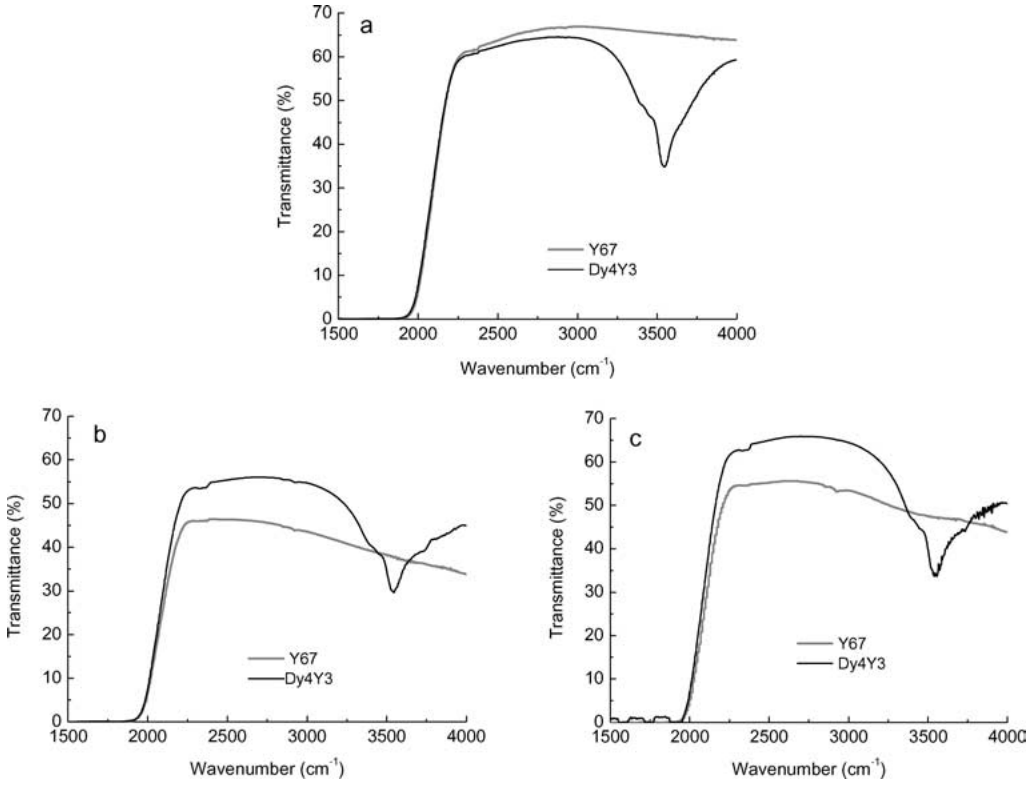

Figure 5 Optical transmittance of Dy4Y3 and Y67 specimens (0.5 mm in thickness): (a) SPS-ed, (b) after 7 h heat treatment and (c) after 17 h heat treatment.

maximum value of transmittance of SPS-ed Dy4Y3 was about 64%, and SPS-ed Y67 had a slightly higher optical transmittance at 66%. There is an absorption peak at about 3540 cm^{-1} on the transmittance curve of Dy4Y3 that corresponds to the $^6H_{15/2} \rightarrow {}^6H_{11/2}$ electron transition of Dy^{3+}. A 7 h heat treatment caused a decrease in optical transmittance for both samples, as shown in Fig. 5b, and the maximum optical transmittance of Dy4Y3 (56%) was higher than that of Y67 (47%). With 17 h heat treatment, the optical transmittance of both samples increased, to 66 and 56% for Dy4Y3 and Y67 respectively (see Fig. 5c)).

It is well known that the main factors affecting optical transmittance of polycrystalline ceramics are density, phase assemblage, microstructure and uniformity of the material [19]. There was no appreciable change in the bulk densities of SPS-ed samples with and without heat treatment (see Table I), suggesting that the density is not a very important factor to influence the optical transmission of samples in the present work. As mentioned above, there are some differences in SEM images between Dy4Y3 and Y67 after SPS, although both samples consisted of single α' phase. More grain boundary glassy phase was observed in Dy4Y3 than in Y67. The fact that the optical transmittances of SPS-ed Dy4Y3 and Y67 samples were similar implies that the constituents of the grain boundary phase did not seem to affect the optical transmission for the specimens without heat treatment. After heat treatment for 7 h, the crystalline melilite phase formed in both samples, and the content was higher in Y67 than in Dy4Y3. This may result in a change in refractive index of the intergranular phase because of both the formation of melilite and the change in the constituents of the grain boundary in the samples. The 7 h heat treatment also produced the bimodal microstructure as shown in Fig. 4b, in which some α' grains grew as a result of some smaller grains being consumed, thus resulting in the inhomogeneous distribution of grains sizes. The decrease in optical transmittance is therefore attributed to the formation of melilite phase and inhomogeneous microstructure in the materials.

As the heat treatment time prolonged to 17 h, the amount of melilite phase in Y67 was unchanged, but most α' grains developed an equi-axed morphology and the distribution of grain size became more homogeneous than that following the 7 h heat treatment. The increased optical transmittance of Y67 from 47 to 56% when heat treated for 17 h is attributed to the improved microstructure and slightly increased density. The transmittance of Dy4Y3 was consistently higher than that of Y67 under both heat treatment conditions. This may be related to the rare earth ion distribution in α' grains and intergranular phase, as Dy^{3+} were mainly incorporated into α' structure, while all Y^{3+} existed in the melilite and intergranular phase. The contribution of decreased amount of melilite in Dy4Y3 after 17 h heat treatment to the increased transmittance is also noted.

4. Conclusions

Fully densified specimens consisting of single crystalline α-sialon phase could be obtained by spark plasma sintering with $Y_{0.67}Si_9Al_3ON_{15}$ and $Dy_{0.4}Y_{0.3}Si_{8.85}Al_{3.15}O_{1.05}N_{14.95}$ compositions. The SPS-ed samples had relatively high optical transmission properties, and the maximum transmittance for 0.50 mm thick samples reached about 65% in 4000–1500 cm^{-1} wave numbers. After heat treatment for 7 h, the optical transmittances of both samples decreased. However, the transmittance of $Dy_{0.4}Y_{0.3}Si_{8.85}Al_{3.15}O_{1.05}N_{14.95}$ was increased to the same level as before treatment by the extending the heat treatment time to 17 h. The transmittance of $Y_{0.67}Si_9Al_3ON_{15}$ was lower than its counterpart $Dy_{0.4}Y_{0.3}Si_{8.85}Al_{3.15}O_{1.05}N_{14.95}$ under the same heat treatment condition.

In α-sialon systems, the distribution of size and shape of α-sialon grains, amount and constituents of grain boundary glassy phase, and the second crystallized phase, are key factors affecting the optical transmission of samples. Better optical transmission properties can be obtained from materials with homogeneous microstructure and grains with equi-axed α-sialon grain morphology.

The results reveal that α-sialon ceramics with high transmittance at infrared wavelengths could be as a promising infrared window material used at high temperature or under severe conditions, combined with its excellent mechanical properties.

Acknowledgments

This work was supported by The Outstanding Overseas Chinese Scholars Fund of Chinese Academy of Sciences (2001-1-12) and National Natural Sciences Foundation of China.

References

1. S. HAMPSHIRE, H. K. PARK, D. P. THOMPSON and K. H. *Nature* **274** (1978) 880.
2. Z. K. HUANG, W. Y. SUN and D. S. YAN, *J. Mater. Sci. Lett.* **4** (1985) 255.
3. D. P. THOMPSON, *Mater. Sci. Forum* **47** (1989) 21.
4. D. STUTZ, P. GREIL and G. PETZOW, *J. Mater. Sci. Lett.* **5** (1986) 335.
5. B. S. M. KARUNARATNE, R. J. LUMBY and M. H. LEWIS, *J. Mater. Res.* **11** (1996) 2790.
6. H. MANDAL, *J. Eur. Ceram. Soc.* **19** (1999) 2349.
7. Z. J. SHEN, M. NYGREN and U. HALENIUS, *J. Mater. Sci. Lett.* **16** (1997) 263.
8. K. E. JOHANSSON, T. PALM and P. -E. WERNER, *J. Phys. E. Sci. Instrum.* **13** (1980) 1289.
9. P.-E. WERNER, *Arkiv fur Kemi.* **31** (1964) 513.
10. Z. J. SHEN, Z. ZHAO, H. PENG and M. NYGREN, *Nature* **417** (2002) 266.
11. J. ZHANG, A. ZAVALIANGOS, M. KRAEMER and J. GROZA, in Proceedings of a Symposium on Modelling the Performance of Engineering Structural Materials III, Columbus, Oct. 2002, edited by T. S. Srivatsan, D. R. Lesuer and E. M. Taleff (Minerals, Metals & Materials Society, Warrendale, 2002) p. 299.
12. Z. J. SHEN, H. PENG and M. NYGREN, *J. Amer. Ceram. Soc.,* in press.
13. W. Y. SUN, T. Y. TIEN and T. S. YEN, *ibid.* **74** (1991) 2547.
14. D. P. THOMPSON, P. KORGUL and A. HENDRY, "Progress in Nitrogen Ceramics" (Martinus Nijhoff, The Hague, The Netherlands, 1983) p. 61.
15. Z. K. HUANG, Y. Z. JIANG and T. Y. TIEN, *J. Mater. Sci. Lett.* **16** (1997) 747.
16. C. J. HWANG, D. W. SUSNITZKY and D. R. BEAMAN, *J. Amer. Ceram. Soc.* **78** (1995) 588.
17. P. L. WANG, C. ZHANG, W. Y. SUN and D. S. YAN, *Mater. Lett.* **38** (1999) 178.
18. P. L. WANG, J. H. ZHANG, J. B. HE and D. S. YAN, *J. Eur. Ceram. Soc.* **20** (2000) 1987.
19. M. FOX, "Optical Properties of Solids" (Oxford University Press Inc., New York, 2001) p. 8.

Received 14 July 2003
and accepted 11 May 2004